Steel and Composite Structures, *Vol. 18*, *No. 3* (*2015*) *603-621*
DOI: http://dx.doi.org/10.12989/scs.2015.18.3.603

On the evaluation of critical lateral buckling loads of prismatic steel beams

R. Aydin *, A. Gunaydin and N. Kirac

Department of Civil Engineering, *Eskisehir Osmangazi University*, *Eskisehir*, *Turkey*

(*Received October 18*, *2010*, *Revised August 17*, *2014*, *Accepted August 29*, *2014*)

Abstract. In this study, theoretical models and design procedures of the behavior of thin-walled simply supported steel beams with an open cross section under a large torsional effect are presented. I-sections were chosen as the cross section types. Firstly, the widely used differential equations for the lateral buckling for the pure bending moment effect in a beam element were adopted for the various moment distributions along the span of the beam. This solution was obtained for both mono-symmetric and bisymmetric sections. The buckling loads were then obtained by using the energy method. When using the energy method to solve the problem, it is possible to locate the load not only on the shear center but also at several points of the section depth. Buckling loads were obtained for six different load types. Results obtained for different load and cross section types were checked with ABAQUS software and compared with several standard rules.

Keywords: lateral torsional buckling; I-section beams; stability; buckling load

1. Introduction

Steel beams are usually bent in the plane of greater rigidity, so the flexural rigidity on the major principal axis of the beam is many times larger than that on the minor axis. One of the failure modes in a compact steel beam subjected to a bending moment with respect to its major principal axis is lateral torsional buckling in which the beam is bent in the bending plane, buckled in a plane perpendicular to the bending plane and twisted. The lateral torsional buckling will gain in importance when the beam is not laterally constrained. The geometric properties of the section, load types and the point at which the load is applied are the basic parameters affecting the critical lateral buckling load.

Differential equations which are obtained for the critical lateral buckling load of a beam subjected to pure bending about its major principal axis can be solved analytically by considering the end conditions of the beam. But if the moment varies along the beam, then the analytical solution is more complex. In addition, it must be assumed that the loads which produce moments are applied through the shear center of the beam, otherwise second-order torsion effects can be formed on the beam but their effects cannot be considered theoretically. Steel beams can be loaded on various locations of the beam cross section depth like the center of gravity, top or bottom flange. The applicability of the method is restricted, because the effects of these different loading cases

*Corresponding author, Professor, E-mail: raydin@ogu.edu.tr

http://www.techno-press.org/?journal=scs&subpage=8 ISSN: 1229-9367 (Print), 1598-6233 (Online)

cannot be considered.

Another method is to use energy equations. In this method, related equations can be obtained by considering second-order effects. But an assumption must be also made about the displacement function that satisfies the end conditions. Related results are acceptable if the displacement function is in accordance with the real displacement values. The displacement function is generally chosen to be symmetrical about the beam center. The compatibility of the function must be checked for non-symmetric loading cases.

In the present study, firstly, the differential equations for a mono- and bisymmetric I-section simply supported steel beam subjected to pure bending are solved. The solution is then extended to six different load types along the beam span. While these extensions were made, it is accepted that the beam is divided into finite segments and the bending moment for each segment is assumed to be constant. For a simply supported beam and a certain external load value a set of homogenous linear equations will be obtained. The critical buckling load case can be obtained for the external load value at which the determinant of the coefficient matrix of these linear homogenous equations vanishes.

Analyses are also made by using the energy method for the same load types. Numerical solutions of certain integral expressions which occur in calculating for the work done by the external load during lateral buckling were determined by Simpson integration rule (Atkinson 1989). A closed form solution of these integral expressions is very difficult for each load type. Therefore, a numerical solution should be more advantageous.

Comparisons were made for the results obtained from ABAQUS (2008) software and analytical calculations for various load and cross section types.

The first known studies on the topic of lateral buckling of beams were the Ph.D. thesis by Prandtl and the study by Michell (Torkamani and Roberts 2009), in which they considered only the buckling of beams with narrow rectangular cross sections. Both of these studies were published in 1899. Their work was further enhanced by that of Timoshenko and Gere (1961), Bleich (1952) and Trahair (1977). This research was then extended to include wide flange sections, and it was published in textbooks. Specifications for considering lateral buckling in design was first released in 1976 (CRC 1976). Buckling problems can also be solved by applying techniques in the standard calculus of variations. In these techniques, Vlassov's (Vlassov 1961) classical hypothesis of the thin-walled beam theory was used (Trahair 1993). Nethercot (1983) and Trahair and Bradford (1998) investigated the solution of the differential equation of a beam for certain support conditions by accepting a half-sine wave as the displacement function. The finite integral method was developed by Brown and Trahair (1968) for the solution of the differential equation and was applied successfully to a number of buckling problems. Elastic and inelastic buckling problems solved by applying the finite integral method have been the subject of many articles in the literature. In the studies of I-beams conducted by Kitipornchai and Richter (1978), Kitipornchai and Trahair (1975) and Kitipornchai *et al*. (1984, 1986), various load types, support conditions and stress cases were examined.

If we prefer energy methods for achieving stability analyses, the Rayleigh-Ritz (Timoshenko and Gere 1961) and Galerkin methods (Mohri *et al*. 2003) are two successful methods for computing analytical solutions for buckling loads. Studies by Torkamani and Roberts (2009), Mohri *et al*. (2003, 2008a, b, 2010), Andrade *et al*. (2007), Larue *et al*. (2007) and Lim *et al*. (2003) are important studies concerning the energy methods. In these studies the obtained results by the energy method are also compared with results from the use of the finite element method, the finite difference method and code specifications.

By using computer technology, successful analytical analyses can be made for solving buckling problems. Some research was carried out by using the finite element, the finite difference or the finite strip method by Park *et al*. (2004), Suryoatmono and Ho (2002), Aktas (2005), Serna *et al*. (2006), Zirakian (2008, 2010), Taras and Greiner (2008) and Bui (2009). Some software applicable to the finite element method was used by Lim *et al*. (2002) and Aydin and Dogan (2007) especially for solving buckling problems. ABAQUS (2008) software, developed for computing general structural analysis problems, also can be used for solving buckling problems. Design rules are given in the codes, e.g., EC3 (2005a), AISC Specification (2005a) and BS5950-1 (2000). Similar rules are also given in the SSRC guide (Galambos 1998).

2. Lateral buckling of simply supported beams subjected to pure bending about the major principal axis

Here, the mono-symmetric or bisymmetric I-section simply supported beam which is subjected to pure bending or various load types is considered.

2.1 Mono-symmetric I-section simply supported beam under pure bending

Fig. 1 shows the lateral buckling of a mono-symmetric I-section simply supported beam subjected to pure bending. Positive directions are assumed for the axes, bending moment, M_x, displacements and twist angle as shown in Fig. 1. Lateral buckling equations for the beam are given below (Timoshenko and Gere 1961)

$$EI_y \frac{d^4u}{dz^4} - M_x \frac{d^2\phi}{dz^2} = 0 \tag{1}$$

$$EC_w \frac{d^4\phi}{dz^4} - (GJ - \beta_x M_x)\frac{d^2\phi}{dz^2} - M_x \frac{d^2u}{dz^2} = 0 \tag{2}$$

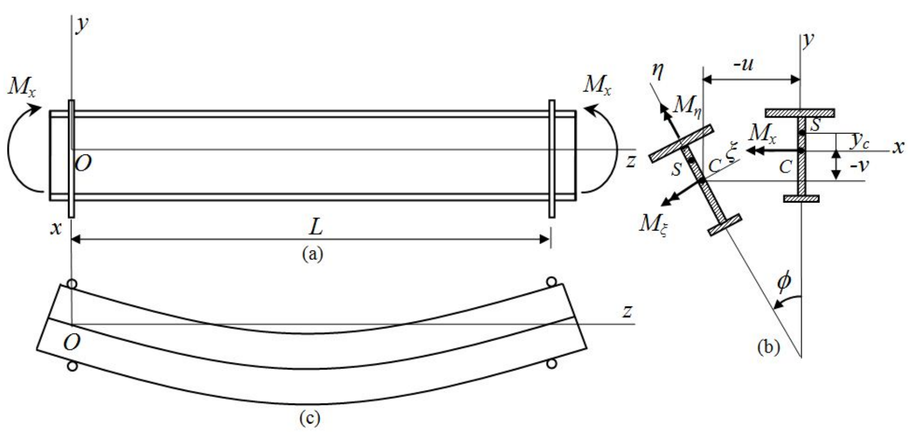

Fig. 1 (a) Lateral buckling of mono-symmetric I-beam subjected to pure bending; (b) cross section; (c) deformed shape where

EI_y = bending rigidity about the y-axis
GJ = torsional rigidity
EC_w = warping rigidity
ϕ = twist angle

$$\beta_x = \frac{1}{I_x}\int_A y(x^2 + y^2)dA - 2y_c \tag{3}$$

where

β_x = the Wagner coefficient
y_c = the coordinate of the shear center, according to the coordinate system passing through the center of gravity, C (see Fig. 1(b))

By differentiating Eq. (2) twice with respect to z and substituting into Eq. (1) we obtain

$$\frac{d^6\phi}{dz^6} - \left(\frac{GJ - M_x\beta_x}{EC_w}\right)\frac{d^4\phi}{dz^4} - \frac{M_x^2}{EC_w EI_y}\frac{d^2\phi}{dz^2} = 0 \tag{4}$$

In this paper, the following function is assumed for the solution of Eq. (4)

$$\phi = A_1 \cos Dz + A_2 \sin Dz \tag{5}$$

By substituting Eq. (5) into Eq. (4) we obtain

$$D^6 + 2\left(\frac{GJ - M_x\beta_x}{2EC_w}\right)D^4 - \frac{M_x^2}{EC_w EI_y}D^2 = 0 \tag{6a}$$

or

$$D^2\left[D^4 + 2\left(\frac{GJ - M_x\beta_x}{2EC_w}\right)D^2 - \frac{M_x^2}{EC_w EI_y}\right] = 0 \tag{6b}$$

2.2 Bisymmetric I-section simply supported beam under pure bending

Equation systems for bisymmetrical cross sections are simpler than Eq. (4). For this case the related equation is

$$EC_w\frac{d^4\phi}{dz^4} - GJ\frac{d^2\phi}{dz^2} - \frac{M_x^2}{EI_y}\phi = 0 \tag{7}$$

If we assume the same function for the twist angle, ϕ, which is defined in Eq. (5), we obtain

$$D^4 + 2\frac{GJ}{2EC_w}D^2 - \frac{M_x^2}{EC_w EI_y} = 0 \tag{8}$$

Eqs. (6b) and (8) are the similar type equations. D^2 values which satisfy both equations are given below

$$D^2 = -\alpha + \sqrt{\alpha^2 + \delta} \tag{9}$$

where, for the mono-symmetric case

$$\alpha = \frac{GJ - M_x \beta_x}{2EC_w} \tag{10a}$$

for the bisymmetric case

$$\alpha = \frac{GJ}{2EC_w} \tag{10b}$$

and

$$\delta = \frac{M_x^2}{EC_w EI_y} \tag{10c}$$

As can be seen from these equations, the solutions are similar for the mono-symmetric and bisymmetric cases. In the mono-symmetric case torsional rigidity decreases by $M_x\beta_x$ when compared with the torsional rigidity of the bisymmetric case [see Eqs. (10a) and (10b)]. But the δ values are the same for both cases.

If the shear center is in compression, the Wagner coefficient given in Eq. (3) has a negative value with respect to the coordinate system (see Fig. 1(b)). In other words, the torsional rigidity increases in this case.

3. Mono-symmetric or bisymmetric I-section simply supported beam, various moment distributions along beam span

A simply supported beam loaded parallel to the vertical axis, y, allows us to use Eqs. (4) and (7). It is assumed that the beam is divided into finite segments and the bending moment for each segment is assumed to be constant. In this case, with respect to Eq. (5), the constant of integration is twice the value of the segment number. If we consider the related boundary conditions at the nodes of the segments for twist angles which are equal and continuous but zero at the ends of the beam, we can obtain a set of linear equations. The elements of these equations include the bending moments which are assumed to be constant for each segment. The certain value of an external load case that produces the constant assumed flexural moments on each segment which makes the determinant of the coefficient matrix of the linear homogenous equations equal to zero is referred to as the critical lateral torsional buckling load. Using software developed specifically for this study, we obtained solutions for the six different load types shown in Fig. 2. In this study there are 6 load types presented for a simply supported beam which is not restrained along its length laterally except load type 6. Load type 6 represents uniformly distributed load on a beam restrained laterally at intermediate (1/3)L points.

4. Solution using energy method

Using the strain energy method to solve stability problems is more effective than using the

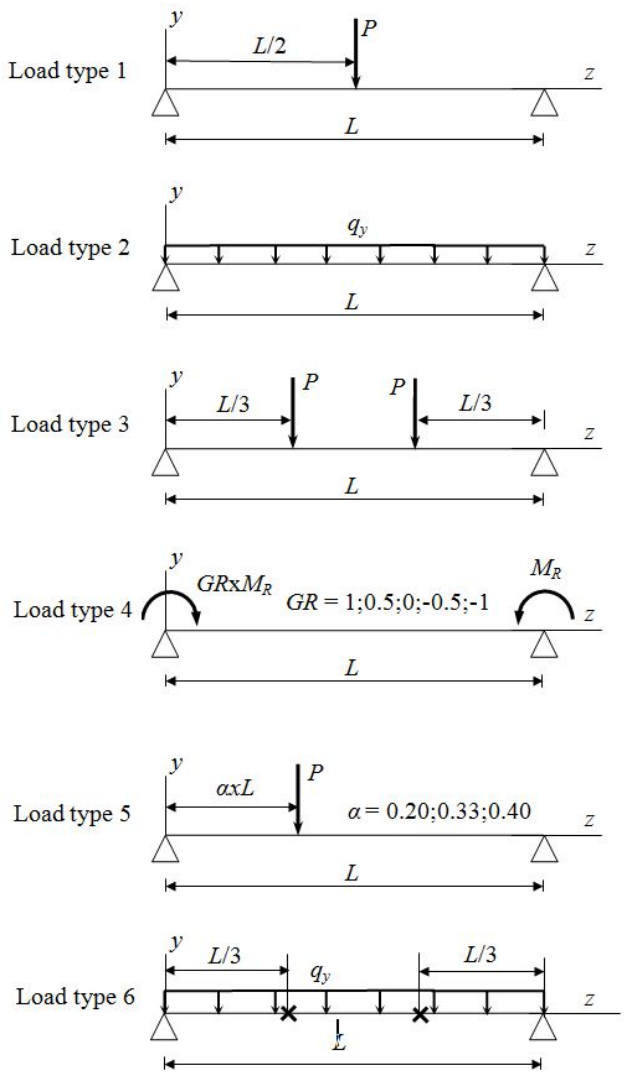

Fig. 2 Load types

differential equation solution method. When the beam buckles laterally, the strain energy increases. To calculate the increase in the strain energy due to torsion and warping, we can use the following expression

$$\Delta U = \int_0^L \frac{(GJ - M_x\beta_x)}{2}\left(\frac{d\phi}{dz}\right)^2 dz + \frac{EC_w}{2}\int_0^L \left(\frac{d^2\phi}{dz^2}\right)^2 dz \tag{11}$$

In Eq. (11), the integrals represent strain energy terms produced by the torsion and warping effects, respectively. In the bisymmetric case it is clear that $M_x\beta_x = 0$.

The component in the η-axis of the bending moment, M_x of a simply supported beam is defined as M_η.

M_η will be taken as the external effect that causes lateral buckling

$$M_\eta = M_x \phi \tag{12}$$

and the corresponding work produced by M_η is

$$W_1 = \frac{1}{2EI_\eta} \int_0^L (M_x \phi)^2 \, dz \tag{13}$$

If the external loads are applied at an out-of-shear center like on the top flange, lowering the application point of the loads causes second-degree effects. So, it is apparent that the critical value of the load is decreased when the point of application is lowered but it is increased when it is raised. The impact of this effect on the critical buckling load can be obtained by using the energy method. It is only necessary to consider the additional lowering or rising of the loads during lateral buckling due to the rotation of the cross section. If H_A is the vertical distance of the point of application of the load from the shear center of the cross section, the lowering of the load is (see Fig. 3)

$$\Delta = H_A (1 - \cos \phi) \approx \frac{\phi^2 H_A}{2} \tag{14}$$

H_A is assumed to be positive when it is above the shear center. Due to Δ, external loads produce additional work

$$W_2 = \frac{H_A}{2} \int_0^L \phi^2 q_y \, dz \tag{15a}$$

where q_y indicates the uniformly distributed load acting along the z-axis. If the forces are concentrated, then we use

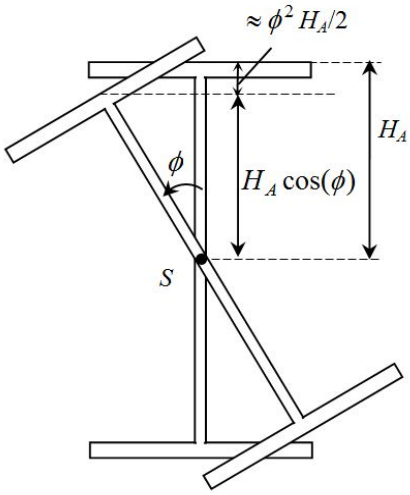

Fig. 3 Lowering of a point of cross section at distance, H_A from shear center during twisting

$$W_2 = \frac{H_A}{2}\sum_{i=1}^{N}\phi_i^2 P_i \tag{15b}$$

where N indicates the number of forces, and ϕ is the twist angle at the point where the load, P is applied. The corresponding work produced by M_η and lowering of the application loads of the external forces can be found from the sum of Eqs. 13 and 15(a) and/or 15(b)

$$\Delta W = W_1 + W_2 \tag{16}$$

The system is stable in its non-deflected form if $\Delta U > \Delta W$, and unstable if $\Delta U < \Delta W$. Thus the critical value of the load is found from the following condition

$$\Delta U = \Delta W \tag{17}$$

So we obtain either

$$W_2 + \frac{1}{2EI_\eta}\int_0^L (M_x\phi)^2\,dz = \int_0^L \frac{(GJ - M_x\beta_x)}{2}\left(\frac{d\phi}{dz}\right)^2 dz + \frac{EC_w}{2}\int_0^L\left(\frac{d^2\phi}{dz^2}\right)^2 dz \tag{18a}$$

or

$$W_2 + \frac{1}{2EI_\eta}\int_0^L (M_x\phi)^2\,dz + \int_0^L \frac{M_x\beta_x}{2}\left(\frac{d\phi}{dz}\right)^2 dz = \frac{GJ}{2}\int_0^L\left(\frac{d\phi}{dz}\right)^2 dz + \frac{EC_w}{2}\int_0^L\left(\frac{d^2\phi}{dz^2}\right)^2 dz \tag{18b}$$

To solve Eq. (18b), a function will be chsen which satisfies the end conditions of the beam. Assuming that the ends of the beam cannot rotate about the z-axis but are free to warp, we find that the conditions at the ends of the beam are

$$\phi = 0 \quad \text{and} \quad \frac{d^2\phi}{dz^2} = 0 \quad \text{at} \quad z = 0 \quad \text{and} \quad z = L \tag{19}$$

The moment value on the top flange is equal to zero at the ends of the beam. Thus, the warping will be equal to zero at these points. This is the reason for the second condition in Eq. (19).

The twist angle, ϕ, could be taken in the form of a trigonometric function for load types 1-5 as follows

$$\phi = A\sin\frac{\pi}{L}z \tag{20a}$$

and for load type 6

$$\phi = A\sin\frac{3\pi}{L}z \tag{20b}$$

Explanations about calculation the integrals of Eq. (18b) will be given for load type 1 and applications for the other load types will be shown later in this paper.

For a concentrated load, P, acting at the middle span (load type 1)

$$W_2 = A^2 P\frac{H_A}{2} \tag{21a}$$

The second and third terms of Eq. (18b) are solved numerically by the Simpson method. This is done by dividing the beam into $N = 24$ equal segments: (number of equal segments must be even). Numerical value of an integral is obtained on the following form with respect to the Simpson method.

$$\int_0^L y dz = \frac{L}{3N}\left[y_0 + y_N + 4\sum_{i=1}^{N-1} y_i + 2\sum_{i=2}^{N-2} y_i \right] \tag{21b}$$

Here y's are the numerical values at the segment end points

$$\frac{1}{2EI_\eta}\int_0^L (M_x\phi)^2 dz = \frac{A^2 (D_1 P^2 L^3)}{2EI_\eta}; \quad D_1 = 16.749\times 10^{-3} \tag{21c}$$

$$\int_0^L \frac{M_x\beta_x}{2}\left(\frac{d\phi}{dz}\right)^2 dz = A^2 (D_2\beta_x P); \quad D_2 = 0.18345 \tag{21d}$$

$$\text{Here} \quad \frac{d\phi}{dz} = A\frac{\pi}{L}\cos\frac{\pi}{L}z \quad \text{and} \quad M_x = \frac{P}{2}z, \quad z \le \frac{L}{2} \tag{21e}$$

Other integral expressions in Eq. (18b) may be obtained in closed form and they are shown below

$$\frac{EC_w}{2}\int_0^L \left(\frac{d^2\phi}{dz^2}\right)^2 dz = A^2\,\frac{\pi^4 EC_w}{4L^3} \tag{21f}$$

$$\int_0^L \frac{GJ}{2}\left(\frac{d\phi}{dz}\right)^2 dz = A^2\,\frac{\pi^2 GJ}{4L} \tag{21g}$$

Substituting Eqs. (21a)-(21g) into Eq. (18b) by eliminating A^2 terms, we obtain

$$\frac{D_1 L^3}{2EI_\eta}P^2 + \left(\frac{H_A + 2D_2\beta_x}{2}\right)P - \frac{\pi^2 GJ}{4L}\left(1 + \frac{\pi^2 EC_w}{L^2 GJ}\right) = 0 \tag{22}$$

When Eq. (22) is solved for P

$$P = \frac{P_{cr}}{2\pi^2 L\sqrt{D_1}}\left[-\frac{kH_A + 2D_2\beta_x}{\sqrt{D_1}} + \sqrt{\frac{(kH_A + 2D_2\beta_x)^2}{D_1} + \frac{2\pi^4 GJ}{P_{cr}}\left(1 + \frac{\pi^2 EC_w}{L^2 GJ}\right)} \right] \tag{23}$$

where

$P_{cr} = \dfrac{\pi^2 EI_\eta}{L^2}$ and (for load type 1 $k = 1$)

Note: For load type 6, 3π must be substituted into Eq. (23) in lieu of π (see Eq. 20(b)).

Eq. (23) can also be applied to other load types. The buckling loads must be in units of force. For example, it is qL for type 2 or M/L for type 4.

Table 1 Coefficients for different loading types [See Eq. (23)]

Load type		Obtained load	D_1	D_2	k
1		P	16.749×10^{-3}	0.18345	1
2		qL	6.0915×10^{-3}	0.14312	0.50
3		P	46.2902×10^{-3}	0.36080	1.5
4	(GR = 1)	M_R / L	0.5	2.46901	-
4	(GR = 0.5)	M_R / L	0.28534	1.85055	-
4	(GR = 0)	M_R / L	0.14134	1.23370	-
4	(GR = –0.5)	M_R / L	0.06801	0.61685	-
4	(GR = –1)	M_R / L	0.06535	0	-
5	(α = 0.20)	P	5.315×10^{-3}	0.15422	0.3455
5	(α = 0.33)	P	12.194×10^{-3}	0.18040	0.75
5	(α = 0.40)	P	14.991×10^{-3}	0.18304	0.9045
6		qL	4.019×10^{-3}	1.78848	0.50

*Notes:

(1) It is assumed that in load type 4, flexural moments are applied on the gravity center of the cross section.

(2) H_A is assumed to be positive when it is above the shear center in Eq. (23).

The kH_A values can be calculated from the integrals of Eqs. (15a) or (15b) and other load types should be converted to load type 1. For example, for load type 2: [comparison with the Eq. (21a)]

$$\frac{H_A}{2}\int_0^L \sin^2\left(\frac{\pi}{L}z\right) q_z dz = \frac{H_A}{4} q_z L = \frac{kH_A}{2} q_z L, \quad k = 0.5 \tag{24}$$

According to Eq. (24), k must be taken as 0.5 when using Eq. (23) for load type 2.

Table 1 lists the values calculated for the k coefficients for the other load types.

5. The ABAQUS model

For finite element modelling, the commercial multipurpose software package ABAQUS (2008) was employed in this research. An eight-node, doubly curved shell element with reduced integration S8R5 was used to model the flanges and webs. S8R5 is a quadrilateral shell element with five degrees of freedom per node (three displacement components and two in-surface rotation components). The computational time and accuracy largely depend on the number of elements and integration points. Mesh studies have indicated that it would be adequate to use eight elements through the depth of the web and four elements across the width of the flange for the I-section. The element sizes along the longitudinal direction are 200 mm. The default integration method is based on Simpson's rule, with five integration points through the thickness of the element. All the end nodes on the web are restrained against displacements in principal axes x and y and rotation around the longitudinal axis z. The loads were applied according the desired loading locations on the top flange-web junction, gravity center or bottom flange–web junction of the I-sections. Eigenvalue

Table 2 Critical lateral buckling moments for section *A* (kN-m)

Load type 2					Load type 5 ($\alpha = 0.2$)				
Span (mm)		Load on top flange	Load on gravity center	Load on bottom flange	Span (mm)		Load on top flange	Load on gravity center	Load on bottom flange
	PS	221.65	315.18	448.18		*PS*	332.08	431.88	561.72
5,000	*ABQ*	219.96	311.03	441.08	5,000	*ABQ*	300.90	409.38	536.37
	PS/*ABQ*	1.01	1.01	1.02		*PS*/*ABQ*	1.10	1.05	1.05
	PS	172.59	238.62	329.90		*PS*	256.83	326.98	416.28
6,000	*ABQ*	173.91	240.81	333.86	6,000	*ABQ*	237.73	319.32	411.59
	PS/*ABQ*	0.99	0.99	0.99		*PS*/*ABQ*	1.08	1.02	1.01
	PS	141.80	191.04	257.38		*PS*	209.68	261.78	326.83
7,000	*ABQ*	144.48	195.79	265.45	7,000	*ABQ*	196.66	260.48	330.62
	PS/*ABQ*	0.98	0.98	0.97		*PS*/*ABQ*	1.07	1.00	0.99
	PS	105.64	136.19	175.56		*PS*	154.51	186.61	225.38
9,000	*ABQ*	109.52	142.65	185.79	9,000	*ABQ*	147.51	190.08	234.84
	PS/*ABQ*	0.96	0.95	0.94		*PS*/*ABQ*	1.05	0.98	0.96
	PS	94.13	119.12	150.76		*PS*	137.04	163.23	194.44
10,000	*ABQ*	98.32	125.88	161.12	10,000	*ABQ*	131.77	167.68	204.75
	PS/*ABQ*	0.96	0.95	0.94		*PS*/*ABQ*	1.04	0.97	0.95
	PS	85.07	105.92	131.87		*PS*	123.34	145.14	170.78
11,000	*ABQ*	89.49	112.82	142.17	11,000	*ABQ*	119.41	150.18	181.47
	PS/*ABQ*	0.95	0.94	0.93		*PS*/*ABQ*	1.03	0.97	0.94
	PS	77.75	95.40	117.07	12,000	*PS*	112.31	130.73	152.17
12,000	*ABQ*	82.34	102.37	127.20		*ABQ*	109.44	136.16	162.99
	PS/*ABQ*	0.94	0.93	0.92		*PS*/*ABQ*	1.03	0.96	0.93

PS: Present Study, *ABQ*: ABAQUS software

analyses were conducted to determine buckling loads. This is a linear elastic analysis performed using the (*BUCKLE) procedure available in ABAQUS (2008).

6. Numerical examples

Numerical examples were solved for two I-section simply supported beams which have a depth h = 400 mm. Other dimensions are given below.

For section *A*:

h = 400 mm, $b = b_1$ = 180 mm, t_w = 8.6 mm, and t_f = 13.5 mm.
Mechanical material properties of the section are: $I_y = 13.142 \times 10^6$ mm^4,
$I_x = 218.765 \times 10^6$ mm^4, E = 210 GPa, Poissons's ratio v = 0.30
J = 377190 mm^4 and $C_w = 490.049 \times 10^9$ mm^6.

For section *B*:

$b_1 = b/2 = 90$ mm and other dimensions are the same as for section *A*.
Mechanical properties of this section are: $I_y = 7.401 \times 10^6$ mm^4, $I_x = 165.327 \times 10^6$ mm^4, $J = 303379$ mm^4, $C_w = 108.90 \times 10^9$ mm^6 and $\beta_x = -278.3$ mm.

The moment values of the above-mentioned sections having spans in the range L = 5,000-12,000 mm are calculated for uniformly distributed load, i.e., load type 2 and concentrated load type i.e., load type 5 and $\alpha = 0.2$ for the gravity center, top flange and bottom flange loading cases. The results are summarized in Tables 2 and 3. The mean ratios, *PS*/*ABQ*, for cross sections *A* and *B* in Tables 2 and 3 are the same for load type 2 where both cross section types are equal to 0.96 and their standard deviations are equal to 0.03. The mean ratios and standard deviation values for load type 5 and $\alpha = 0.2$ are 1.0 and 0.04, for cross section type *A* and 1.01 and 0.03, respectively, for cross section type *B*.

Table 3 Critical lateral buckling moments for section *B* (kN-m)

Load type 2					Load type 5 ($\alpha = 0.2$)				
Span (mm)		Load on top flange	Load on gravity center	Load on bottom flange	Span (mm)		Load on top flange	Load on gravity center	Load on bottom flange
	PS	201.11	272.47	392.31		*PS*	295.91	369.66	488.52
5,000	*ABQ*	198.19	269.19	392.01	5,000	*ABQ*	269.66	354.78	464.93
	PS/*ABQ*	1.01	1.01	1.00		*PS*/*ABQ*	1.10	1.04	1.05
	PS	156.21	204.28	284.78		*PS*	227.82	277.44	357.21
6,000	*ABQ*	156.24	205.92	292.30	6,000	*ABQ*	212.59	274.04	352.33
	PS/*ABQ*	1.00	0.99	0.97		*PS*/*ABQ*	1.07	1.01	1.01
	PS	127.40	161.83	219.17		*PS*	184.49	219.98	276.78
7,000	*ABQ*	128.93	165.64	229.32	7,000	*ABQ*	174.93	221.38	280.16
	PS/*ABQ*	0.99	0.98	0.96		*PS*/*ABQ*	1.05	0.99	0.99
	PS	92.91	112.91	145.79		*PS*	133.13	153.70	186.28
9,000	*ABQ*	96.03	118.45	157.17	9,000	*ABQ*	129.36	158.63	195.90
	PS/*ABQ*	0.97	0.95	0.93		*PS*/*ABQ*	1.03	0.97	0.95
	PS	81.82	97.76	123.79		*PS*	116.77	133.15	158.96
10,000	*ABQ*	85.39	103.67	135.01	10,000	*ABQ*	114.64	138.79	169.57
	PS/*ABQ*	0.96	0.94	0.92		*PS*/*ABQ*	1.02	0.96	0.94
	PS	73.10	86.09	107.16		*PS*	103.97	117.31	138.22
11,000	*ABQ*	77.00	92.22	118.12	11,000	*ABQ*	103.08	123.38	149.29
	PS/*ABQ*	0.95	0.93	0.91		*PS*/*ABQ*	1.01	0.95	0.93
	PS	66.06	76.84	94.23		*PS*	93.69	104.75	122.01
12,000	*ABQ*	70.23	83.12	104.89	12,000	*ABQ*	93.77	111.10	133.25
	PS/*ABQ*	0.94	0.92	0.90		*PS*/*ABQ*	1.00	0.94	0.92

PS: Present Study, *ABQ*: ABAQUS software

Table 4 Critical lateral buckling moments (kN-m) for section *A* and section *B* with a constant span of L = 7,000 mm Load on gravity center

Section *A*			Section *B*		
Load type	Differential equation solution	Energy method solution	Load type	Differential equation solution	Energy method solution
1	230.43	234.98	1	191.84	207.37
2	191.04	192.45	2	161.83	169.57
3	184.81	186.68	3	155.81	164.55
4 ($GR = 0$)	317.28	315.48	4 ($GR = 0$)	272.41	279.17
5 ($\alpha = 0.2$)	261.78	263.93	5 ($\alpha = 0.2$)	219.98	231.85

At the second phase, L = 7,000 mm is taken as a constant value and critical buckling moments are calculated using both the differential equation solution and energy methods. The results are summarized in Table 4. From the numerical values given in Table 4 it can be seen that the values of the energy method solution are larger than the values of the differential equation solution except in one instance. But the difference is approximately 1% and 5% on cross section types *A* and *B*, respectively.

7. Comparison of the presented procedural results with some code specifications

The procedural results obtained from the energy equation solution can be interpreted by comparison with the existing EC3 (2005a) and AISC Specification (2005a) design rules.

7.1 EC3 specifications

The elastic critical moment for lateral torsional buckling of a beam of uniform symmetrical cross section with equal flanges loaded through the shear center and subject to pure bending is given by Eq. (25)

$$M_{cr,0} = \frac{\pi^2 EI_y}{L^2}\sqrt{\left(\frac{C_w}{I_y} + \frac{L^2 GJ}{\pi^2 EI_y}\right)} \tag{25}$$

The standard conditions of restraint at each end of the beam are: (1) restraint against lateral movement; (2) restraint against rotation about the longitudinal axis; and (3) free to rotate on plan. For uniform, doubly symmetric cross sections, loaded through the shear center at the level of the centroidal axis, and with the standard conditions of restraint described above, M_{cr} can be calculated through Eq. (26)

$$M_{cr} = C_1\frac{\pi^2 EI_y}{L^2}\sqrt{\left(\frac{C_w}{I_y} + \frac{L^2 GJ}{\pi^2 EI_y}\right)} \tag{26}$$

where C_1 is the value for transverse or moment gradient loading, which can be determined from given tables. The C_1 values given in the designers' guide to EC3 (2005b) for end moment loading can be approximated by Eq. (27), though other approximations also exist

$$C_1 = 1.88 - 1.40GR + 0.52GR^2 \leq 2.70 \tag{27}$$

7.2 AISC specifications

Based on the AISC specification provisions of Chapter F, for mono- and bisymmetric I-section members when the web satisfies the noncompact limit

$$\lambda_{r,w} = \frac{h}{t_w} \leq 5.70\sqrt{\frac{E}{F_y}} \tag{28}$$

The elastic critical lateral torsional buckling moment is calculated by

$$M_{cr} = F_{cr} S_x \tag{29}$$

where

$$F_{cr} = \frac{C_b \pi^2 E}{(L/r_t)^2}\sqrt{1 + 0.078\frac{J}{S_x h_0}\left(\frac{L}{r_t}\right)^2} \tag{30}$$

S_x = elastic section modulus taken about major principal axis
h_0 = distance between flange centroids
C_b = lateral torsional buckling modification factor, calculated by

$$C_b = \frac{12.5M_{\max}}{2.5M_{\max} + 3M_A + 4M_B + 3M_C} \leq 3.0 \tag{31}$$

where
$M_{\max}$, M_A, M_B, M_C are absolute values of maximum moment; moments are at quarter, centerline and three-quarter points, respectively.

$$r_t = \frac{b}{\sqrt{12\left(h_0/h + a_w d^2/(6h_0 h)\right)}} \tag{32}$$

where

$$a_w = \frac{h_c t_w}{b t_f} \tag{33}$$

h_c = twice the distance from the centroid to the inside face of the compression flange
d = clear distance between flanges less the corner radius

AISC specification recommends taking the square root term in Eq. (30) equal to 1 if the load is applied on the top flange (AISC 2005b). On the other hand, White (2004) gives the following alternative equation in lieu of Eq. (29)

$$M_{cr} = C_b \frac{\pi^2 E I_y}{L^2}\left[\frac{\beta_x}{2} + \sqrt{\left(\frac{\beta_x}{2}\right)^2 + \frac{C_w}{I_y}\left(1 + 0.039\frac{J}{C_w}L^2\right)}\right] \tag{34}$$

7.3 Comparisons with standards

In this section the critical buckling moment is calculated for cross sections *A* and *B* in accordance both with the presented procedure (energy method) and standards; then their results are compared. For this reason a beam of span L = 7,000 mm with material properties E = 200 GPa, ν = 0.30 is considered for load type 4 (moment gradient loading). Obtained results for sections *A* and *B* are shown in Tables 5(a) and (b).

As can be seen in Table 5(a), the obtained critical lateral buckling moments for section *A* by considering Eq. (29) of this study are generally conservative than the results obtained from the AISC code. The other results obtained are very close to each other. However, the obtained critical lateral buckling moments for section *B* by considering Eq. (29) and Eq. (34) are generally in the unconservative region. The ratio of *PS*/*AISC* reaches a value of 28% for *GR* = –1. The results given in Tables 5(a) and (b) for sections *A* and *B* of moment gradient loading are the same as those obtained from the results of equations in references Kitipornchai *et al*. (1986) and Lim *et al*. (2003).

Additionally, for uniformly distributed and concentrated loading types, the critical buckling moments are calculated in accordance with the presented procedure and standard rules for sections *A* and *B*, and then the results are compared. The obtained results for both sections are shown in Table 6.

Table 5(a) Obtained critical buckling moments for section *A* in accordance with the presented procedure and standard rules for load type 4. L = 7,000 mm; E = 200 GPa

GR	1.0	0.5	0	–0.5	–1.0
PS	160.66	212.67	302.18	435.62	444.39
EC3*	160.66	212.66	302.01	434.46	442.20
PS/EC3*	1.00	1.00	1.00	1.00	1.00
AISC**	166.00	207.48	276.65	360.84	377.24
PS/AISC**	0.97	1.03	1.09	1.21	1.18
EC3***	160.66	210.47	302.04	433.78	433.78
PS/EC3***	1.00	1.01	1.00	1.00	1.02

PS :Present Study; * EC3: [Eq. (26) of *PS*] & Table 6.11 (EC3, 2005b);
** AISC: [Eq. (29) of *PS*]; *** EC3: [Eqs. (26-27) of *PS*]

Table 5(b) Obtained critical buckling moments for section *B* in accordance with the presented procedure and standard rules for load type 4. L = 7,000 mm; E = 200 GPa

GR	1.0	0.5	0	-0.5	-1.0
PS	141.41	186.62	259.24	333.12	250.24
AISC*	152.54	190.68	254.23	331.61	346.68
PS/AISC*	0.93	0.98	1.02	1.00	0.72
AISC**	141.44	176.80	235.73	307.48	321.45
PS/AISC**	1.00	1.06	1.10	1.08	0.78

PS: Present Study; * AISC: [Eq. (29) of *PS*]; ** AISC: [Eq. (34) of *PS*]

8. Numerical examples for load type 6 and comparisons

Load type 6 belongs to a uniformly distributed load for a simply supported beam, which is constrained laterally and cannot rotate about the longitudinal axis, z, at intermediate (1/3) L points of the span. The function for the twist angle, ϕ, given in Eq. (20b), was determined for this case. It was also pointed out to take the value 3π instead of π when applying Eq. (23). Because of the above mentioned properties of load type 6, some solved numerical examples were checked with ABAQUS (2008), and their results compared. If a beam is fully laterally restrained at several intermediate points of the span, then the segments between the laterally restrained points should usually be considered as a simply supported beam under the effect of a moment gradient (EC3 2005b). In this section, some solutions are obtained with acceptance of a simply supported beam under the effect of both a moment gradient and a uniformly distributed load, with recommendations

Table 6 For sections A and B obtained critical buckling moments in accordance with the presented procedure and standard rules for the load types 1 and 2. L = 7,000 mm; E = 200 GPa

Load type	1		1		2		2	
Section type	*A*		*B*		*A*		*B*	
Location	Gravity center	Top flange	Gravity center	Top flange	Gravity center	Top flange	Gravity center	Top flange
PS	219.45	153.54	182.75	136.56	181.94	135.05	154.12	121.34
AISC*	218.40	140.88	200.71	136.38	182.61	121.67	173.34	118.05
PS/ AISC*	1.00	1.09	0.91	1.00	1.00	1.11	0.89	1.03
AISC**	211.44	-	186.10	-	182.61	-	160.73	-
PS/ AISC**	1.04	-	0.98	-	1.00	-	0.96	-
EC3***	219.30	-	-	-	181.87	-	-	-
PS/ EC3***	1.00	-	-	-	1.00	-	-	-

PS :Present Study; * AISC: [Eq. (29) of *PS*]; ** AISC: [Eq. (34) of *PS*];
*** EC3: [Eq. (26) of *PS*] & Table 6.12 (EC3, 2005b)

Table 7 Obtained critical uniform distributed load values, q_{cr}, for a simply supported beam with spans L = 9,000 mm and 12,000 mm and E = 200 GPa under the effect of load type 6 using ABAQUS software, present study and also under the acceptance of the effect of moment gradient between the restrained points

Section type	*A*	*A*	*B*	*B*
Span length (mm)	9,000	12,000	9,000	12,000
ABQ	80.58	27.89	74.84	25.56
PS	86.37	29.50	77.81	26.35
ABQ/*PS*	0.93	0.95	0.96	0.97
SSB 1/3*L*	62.85	21.47	58.15	19.64
ABQ/*SSB* (1/3)*L*	1.28	1.30	1.29	1.30

PS: Present Study; *ABQ*: ABAQUS software; *SSB* (1/3)*L*: Simply supported beam restrained at intermediate (1/3)*L* points of the span under the effect of moment gradient between the restrained points recommendations made about the results. The section types and their properties are identical with previously adopted sections *A* and *B*. The obtained critical buckling load values q_{cr} are tabulated in Table 7 for beam spans L = 9,000 and 12,000 mm, with E = 200 GPa.

As can be seen from Table 7, the results of the present study are about 5% unconservative with respect to ABAQUS software. But the results for the acceptance of the effect of moment gradient between the restrained points are about 30% conservative with respect to ABAQUS software.

9. Conclusions

In the case of a varying moment along the beam, the results obtained by using the assumptions made in this study are reasonable when compared with the results obtained by the energy method and by using ABAQUS software. When using the energy method, a displacement function must be chosen, which is usually symmetric about the beam axis. To understand the effect of a non-symmetric case, an extreme load type (load type 5 and α = 0.2) is chosen, and it is seen that the results are substantially correct. We compared the results obtained for the numerical examples that were solved by using the presented methods and by using ABAQUS software. The differences between the results obtained for the mono- and bisymmetric cross sections are not significant. In the study, both the differential equation and the energy method solutions are approximate calculation procedures, because they have different initial assumptions. Thus, using the procedures mentioned above, we cannot obtain identical results. As can be seen from Table 4, which consists of the numerical example results, the results obtained from both methods are very close. The energy method solutions are usually larger than the differential equation solutions, however.

Load type 6 acts on a beam that has different restraining properties with respect to the other load types. For this load type, the acceptance of a simply supported beam, with its span equal to the distance between the lateral restraint points, and under the effect of a moment gradient loading, give more conservative results. Additionally, as presented in this study, being able to consider loadings out of the shear center of the cross section constitutes an advantage in the design for load type 6.

References

ABAQUS (2008), *Theory Manual*, Version 6.8-2, Hibbit, Karlsson & Sorensen.

AISC (2005a), *Specification for Structural Steel Buildings*, American Institute of Steel Construction, Chicago, IL, USA.

AISC (2005b), *Commentary on the Specification for Structural Steel Buildings*, American Institute of Steel Construction, Chicago.

Aktas, M. (2005), "Verification of nonlinear finite element modelling of I-shaped steel beams under combined loading", *J. Inst. Sci. Tech. Sakarya U.*, **9**(1), 22-29.

Andrade, A., Camotim, D. and Providência e Costa, P. (2007), "On the evaluation of elastic critical moments in doubly and singly symmetric I-section cantilevers", *J. Constr. Steel Res.*, **63**(7), 894-908.

Atkinson, K.E. (1989), *An Introduction to Numerical Analysis*, John Wiley & Sons, New York, NY, USA.

Aydin, R. and Dogan, M. (2007), "Elastic, full plastic and lateral torsional buckling analysis of steel single-angle section beams subjected to biaxial bending", *J. Constr. Steel Res.*, **63**(1), 13-23.

Bleich, F. (1952), *Buckling Strength of Metal Structures*, McGraw Hill, New York, NY, USA.

Brown, P.T. and Trahair, N.S. (1968), "Finite integral solution of differential equations", *Civil Eng. Trans.*, **10**(2), 193-196.

BS5950-1 (2000), *Structural Use of Steelwork in Buildings*, Code of Practice for Design; Rolled and Welded Sections, British Standards Institution, London.

Bui, H.C. (2009), "Buckling analysis of thin-walled sections under general loading conditions", *Thin-Wall. Struct.*, **47**(6-7), 730-739.

CRC (1976), *Guide to Design Criteria for Metal Compression Members*, (3rd Edition), Column Research Council, New York, NY, USA.

EC3 (2005a), EN 1993-1-1; Eurocode 3: *Design of Steel Structures-Part 1-1*: *General Rules and Rules for Buildings*, European Committee for Standardization, Brussels, Belgium.

EC3 (2005b), Designers' Guide to en 1993-1-1; Eurocode 3: *Design of Steel Structure*. *General Rules and Rules for Buildings*, The Steel Construction Institute.

Galambos, T.V. (1998), *Guide to Stability Design Criteria for Metal Structures*, John Wiley & Sons, New York, NY, USA.

Kitipornchai, S. and Richter, N.J. (1978), "Elastic lateral buckling of I-beams with discrete intermediate restraints", *Civil Eng. Trans.*, **20**(2), 105-111.

Kitipornchai, S. and Trahair, N.S. (1975), "Buckling of inelastic I-beams under moment gradient", *J. Struct. Div.* ASCE, **101**(ST5), 991-1004.

Kitipornchai, S., Dux, P.F. and Richter, N.J. (1984), "Buckling and bracing of cantilevers", *J. Struct. Div. ASCE*, **110**(9), 2250-2262.

Kitipornchai, S., Wang, C.M. and Trahair, N.S. (1986), "Buckling of monosymmetric I-beams under moment gradient", *J. Struct. Eng. ASCE*, **112**(4), 781-799.

Larue, B., Khelil, A. and Gueury, M. (2007), "Elastic flexural-torsional buckling of steel beams with rigid and continuous lateral restraints", *J. Constr. Steel Res.*, **63**(5), 692-708.

Lim, N.H., Kim, Y.J. and Kang, Y.J. (2002), "Lateral–torsional buckling of single-axis symmetric I-beams", *J. Civil Eng.* KSCE, **22**(4-A), 871-883.

Lim, N.H., Park, N.H., Kang, Y.J. and Sung, I.H. (2003), "Elastic buckling of I-beams under linear moment gradient", *Int. J. Solids Struct.*, **40**(21), 5635-5647.

Mohri, F., Brouki, A. and Roth, J.C. (2003), "Theoretical and numerical stability analyses of unrestrained, mono-symmetric thin-walled beams", *J. Constr. Steel Res.*, **59**(1), 63-90.

Mohri, F., Bouzerira, C. and Potier-Ferry, M. (2008a), "Lateral buckling of thin-walled beam-column elements under combined axial and bending loads", *Thin-Wall. Struct.*, **46**(3), 290-302.

Mohri, F., Eddinari, A., Damil, N. and Potier-Ferry, M. (2008b), "A beam finite element for non-linear analyses of thin-walled elements", *Thin-Wall. Struct.*, **46**(7-9), 981-990.

Mohri, F., Damil, N. and Potier-Ferry, M. (2010), "Linear and non-linear stability analyses of thin-walled beams with monosymmetric I sections", *Thin-Wall. Struct.*, **48**(4-5), 299-315.

Nethercot, D.A. (1983), "Elastic lateral buckling of beams", In: *Beams and Beam Columns*: *Stability and Strength*, (R. Narayanan Editor), Applied Science Publishers, Barking, England.

Park, J.S., Stallings, J.M. and Kang, Y.J. (2004), "Lateral-torsional buckling of prismatic beams with continuous top-flange bracing", *J. Constr. Steel Res.*, **60**(2), 147-160.

Serna, M.A., Lopez, A., Puente, I. and Yong, D.J. (2006), "Equivalent üniform moment factors for lateral-torsional buckling of steel members", *J. Constr. Steel Res.*, **62**(6), 566-580.

Suryoatmono, B. and Ho, D. (2002), "The moment-gradient factor in lateral-torsional buckling on wide flange steel sections", *J. Constr. Steel Res.*, **58**(9), 1247-1264.

Taras, A. and Greiner, R. (2008), "Torsional and flexural torsional buckling-A study on laterally restrained I-sections", *J. Constr. Steel Res.*, **64**(7-8), 725-731.

Timoshenko, S.P. and Gere, J.M. (1961), *Theory of Elastic Stability*, McGraw Hill, New York, NY, USA.

Torkamani, M.A.M. and Roberts, E.R. (2009), "Energy equations for elastic flexural-torsional buckling analysis of plane structures", *Thin-Wall. Struct.*, **47**(4), 463-473.

Trahair, N.S. (1977), *The Behaviour and Design of Steel Structures*, Chapman & Hall, London, UK.

Trahair, N.S. (1993), *Flexural-Torsional Buckling of Structures*, E&FN Spon, London, UK.

Trahair, N.S. and Bradford, M.A. (1998), *The Behaviour and Design of Steel Structures to AS 4100*, E&FN

Spon, London, UK.
Vlassov, V.Z. (1961), *Thin-Walled Elastic Beams*, National Science Foundation, Washington, D.C., USA.
White, D.W. (2004), "Unified flexural resistance equations for stability design of steel I-section members overview", Structural Engineering, Mechanics and Materials, Report No. 24a; School of Civil and Environmental Engineering, Georgia Institute of Technology, Atlanta, GA, USA.
Zirakian, T. (2008), "Elastic distortional buckling of doubly symmetric I-shaped flexural members with slender webs", *Thin-Wall*. *Struct*., **46**(5), 466-475.
Zirakian, T. (2010), "On the application of the extrapolation techniques in elastic buckling", *J. Const*. *Steel Res*., **66**(3), 335-341.

DL